Clean Energy, 2024, Vol. 8, No. 1, 23–35
https://doi.org/10.1093/ce/zkad084
Advance access publication 2 January 2024
Research Article

Design of a Level-3 electric vehicle charging station using a 1-MW solar system via the distributed maximum power point tracking technique

Afshin Balal* and Michael Giesselmann

Department of Electrical and Computer Engineering, Texas Tech University, Lubbock, TX 79409, USA
*Corresponding author. E-mail: afshin.balal@ttu.edu

Abstract

Solar power is mostly influenced by solar irradiation, weather conditions, solar array mismatches and partial shading conditions. Therefore, before installing solar arrays, it is necessary to simulate and determine the possible power generated. Maximum power point tracking is needed in order to make sure that, at any time, the maximum power will be extracted from the photovoltaic system. However, maximum power point tracking is not a suitable solution for mismatches and partial shading conditions. To overcome the drawbacks of maximum power point tracking due to mismatches and shadows, distributed maximum power point tracking is utilized in this paper. The solar farm can be distributed in different ways, including one DC–DC converter per group of modules or per module. In this paper, distributed maximum power point tracking per module is implemented, which has the highest efficiency. This technology is applied to electric vehicles (EVs) that can be charged with a Level 3 charging station in <1 hour. However, the problem is that charging an EV in <1 hour puts a lot of stress on the power grid, and there is not always enough peak power reserve in the existing power grid to charge EVs at that rate. Therefore, a Level 3 (fast DC) EV charging station using a solar farm by implementing distributed maximum power point tracking is utilized to address this issue. Finally, the simulation result is reported using MATLAB®, LTSPICE and the System Advisor Model. Simulation results show that the proposed 1-MW solar system will provide 5 MWh of power each day, which is enough to fully charge ~120 EVs each day. Additionally, the use of the proposed photovoltaic system benefits the environment by removing a huge amount of greenhouse gases and hazardous pollutants. For example, instead of supplying EVs with power from coal-fired power plants, 1989 pounds of CO_2 will be eliminated from the air per hour.

Received: 25 June 2023. **Accepted:** 15 November 2023

Graphical Abstract

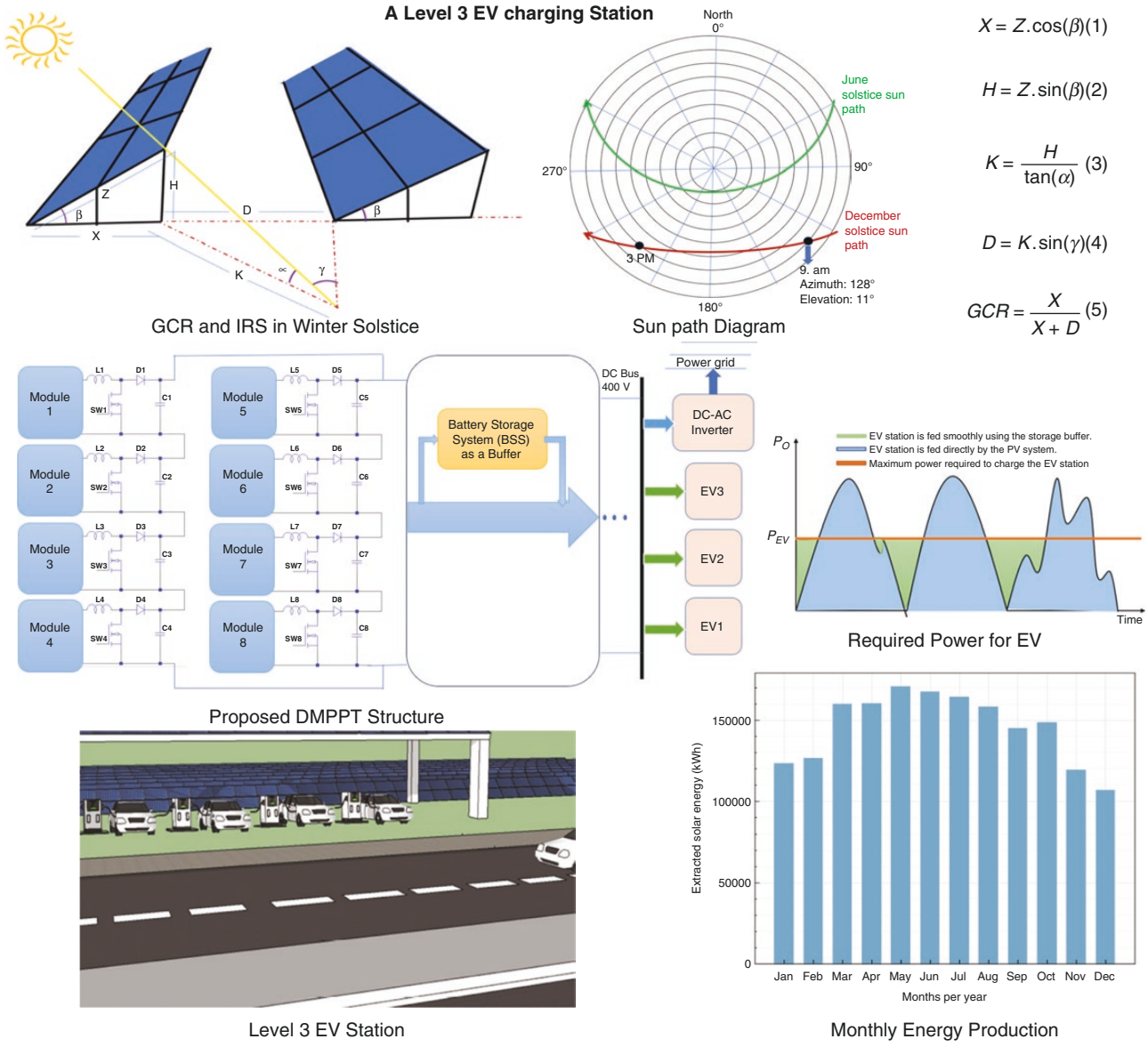

Keywords: electric vehicles (EVs); distributed maximum power point tracking; solar farm; DC fast-charging station; step-up DC–DC converter; System Advisor Model; economic analysis

Introduction

Electric vehicles (EVs) are gaining popularity as a more sustainable and environmentally friendly mode of transportation. Therefore, the demand for EV charging stations is increasing. The use of renewable energy sources, such as solar energy, to power EV charging stations is also becoming more popular. There are three types of EVs on the market, including hybrid EVs, battery electric vehicles (BEVs) and plug-in electric vehicles [1]. With the invention of Level-3 charging stations, an EV can be fully charged in <1 hour [2]. This is an important factor for the acceptance of EVs by a larger demographic. However, the random nature of EV charging demand and the sudden high peak power draw of a Level-3 system put a lot of pressure on the power system [3]. Furthermore, the total energy demand for the projected rate of EV adoption would result in a lack of generation capacity for the existing power grid. Without additional resources, the grid cannot feed EVs and utilizing buffered renewable energies is a solution [4]. Due to the massive energy demand in recent years, renewable energy has grown faster than any other electrical source [5]. In 2020, solar energy represented ~11% of total renewable-energy consumption in the USA [6, 7]. Solar energy, on the other hand, is highly dependent on weather conditions and using maximum power point tracking (MPPT) control methods is essential. One way to increase the efficiency of the system is to use a distributed maximum power point tracking (DMPPT) method that increases output power [8]. As a result, developing a suitable and efficient way to increase efficiency is required. Recently, several studies have been undertaken that have employed solar energy for EV charging stations. In [9], the authors proposed a system for charging stand-alone DC Level-1 EVs using a combination of photovoltaic (PV) panels, grid infrastructure, MPPT

algorithm and the CHAdeMO protocol. The CHAdeMO protocol is a specific fast-charging protocol designed for EVs. CHAdeMO stands for 'CHArge de MOve', which translates into 'charge for moving' in Japanese. This protocol was developed by a consortium of Japanese companies and organizations with the aim of providing fast and efficient charging for EVs. The article described the design and implementation of the proposed system, which can charge an EV using both grid power and solar power, depending on the availability and cost of electricity. The authors also discussed the integration of the CHAdeMO protocol, which is a standardized communication protocol for DC fast charging of EVs. The proposed system allows the integration of the CHAdeMO protocol, allowing compatibility with a wide range of EV models. The results showed that the system can provide a reliable and efficient charging solution for EVs using a combination of grid and solar power. The authors in [10] proposed a novel approach to designing an EV charging station that used both solar and wind power and integrated vehicle-to-grid (V2G) technology. The authors presented a comprehensive system design that included a solar panel array, a wind turbine, a battery energy storage system, an EV charging station and a V2G interface. The system was designed to not only charge EVs, but also feed excess power back into the grid during periods of high demand. The authors concluded that the proposed system could provide reliable and sustainable energy for both EV charging and grid support. The authors in [11] proposed a design for an EV charging station that was supplied by PV energy. The authors also presented a mathematical model of the charging station and used simulation software to analyse the performance of the system under variable conditions. The results of the simulations showed that the proposed charging station was capable of meeting the charging requirements of an EV while operating independently of the power grid. The authors in [12] proposed a design for an EV charging station powered by solar PV energy. The paper described the design of a PV array, a DC–DC converter and the use of a perturb and observe (P&O) algorithm to improve the efficiency of the charging process. The simulation results showed that the charging station was capable of providing efficient and reliable charging for EVs. In [13], the authors presented a study on the feasibility of a hybrid system combining solar and wind power to generate electricity for a grid-connected EV charging station. The study included a system simulation using HOMER software, which allowed the optimization of the system design by finding the optimal combination of solar and wind resources, energy storage capacity and EV charging load. The results indicated that the designed hybrid system was technically feasible with a reasonable payback period. The paper also discussed the potential benefits of the hybrid system, such as improving energy security, reducing greenhouse gas (GHG) emissions and enhancing local economic development through the creation of green jobs. The authors in [14] proposed a control strategy that ensured stable operation of the charging station while maximizing the utilization of renewable energy sources. The control strategy involved a hierarchical control structure that included a primary control loop that smoothed the voltage and current of the converter and a secondary control loop that optimized the power flow between the different energy sources based on the available energy and the EV charging demand. In [15], the author suggested a comparison of the two different DMPPT PV systems, the full power processing (FPP) and differential power processing (DPP) topologies. The DPP topology improved inherent fault tolerances for the entire system from an efficiency standpoint and significantly reduced the cost of power converters by electronically processing only a fraction of the power of the PV panel, which resulted in a significant increase in the efficiency of PV systems in the future. The author in [16] improved the miniaturization, cost and complexity reduction capabilities of the DPP converter and it served as a useful model for the combination of hardware and PV submodule. According to simulation studies in [17], using DMPPT instead of a bypass diode resulted in an ~20% increase in the extracted PV power for higher levels of shading (central MPPT technique). DMPPT is more difficult and expensive to implement than the bypass diode approach. The authors of [18] used a three-level boost converter to integrate PV power into a rapid-charging station for EVs employing PV panels and a battery bank. Although the output capacitor voltage balance must be taken into account, this allowed switching devices to be less strained. The core concept of [19] was using the electric railway power system to feed loads such as EVs with a hybrid system, with the storage and primary power grid serving as a backup. This study designed a solar farm using the DMPPT method that can feed the power grid and charge all kinds of EVs at the same time using a DC fast-charging station.

The objective of this paper is to model a DC fast-charging station employing a 1-MW solar farm with the DMPPT technique, which is significant for several reasons. Overall, this paper represents a significant contribution to achieving a sustainable and zero-emission transportation system. First, this paper addresses one of the major challenges in the widespread adoption of EVs—the availability of fast and convenient charging stations. The use of solar energy to power EV charging stations not only provides a clean and renewable source of energy, but also reduces the dependence on the electric grid, thus increasing the reliability of the charging infrastructure. Second, the use of a DMPPT technique in the study ensures maximum power output from solar panels. This technique allows real-time tracking of the maximum power point (MPP) of the solar panels, ensuring that the charging station operates at maximum efficiency throughout the day. Finally, the study provides a blueprint for the design and construction of a DC fast EV charging station using a 1-MW solar system, which can be replicated and scaled up to meet the increasing demand for an EV charging infrastructure around the world. The structure of this paper is as follows. The methodology, system configuration, ground cover ratio, inter-row spacing, feedback control system, Level-3 charging station and battery storage system (BSS) are explained in Section 1. The simulation results are shown in Section 2. Finally, in Section 3, the conclusion is drawn and explained.

1 Project approach

The technique and materials used for the analysis are covered in this part. These include the mathematical relationships used for the research, the financial and technological elements taken into account for the simulation and the meteorological conditions. Finding the maximum shadowing at the potential site for the solar farm is a crucial step in the planning process. The maximum shadowing condition for the entire year must be determined by calculating the ground coverage ratio (GCR) and inter-row spacing (IRS). DMPPT is utilized to track the MPP and extract the highest amount of solar energy. The MPP of the power–voltage (*P*–*V*) curve can change due to partial shadowing, mismatches and temperature changes. A DMPPT has been proven to improve the efficiency of PV systems. By using the DMPPT technique, it is possible to lower the output power loss caused by improper PV module operation conditions. To correctly track the MPP, a variety

of MPPT techniques can be used. The P&O technique is used in this paper because of its accuracy and fast-tracking characteristic. Furthermore, due to the intermittent nature of PV energy, a BSS is necessary in addition to a solar system in order to provide a stable output from the intended 1-MW PV system. The BSS of the proposed system can provide a 1-hour buffer using 48-V/200-Ah batteries with a depth of discharge (DoD) set at 0.5. A simulation program called the System Advisor Model (SAM) was used to evaluate the output power of the PV system. The data obtained from SAM, covering 1 year, included hourly values of solar radiation (in W/m²), wind speed (in m/s), humidity (in %), rainfall (in inches) and temperature (in °C), covering the entire year to comprehensively assess system performance under different weather conditions, seasons and times of the day. The SAM software itself includes internal data that are used for simulations [20]. Furthermore, to adequately feed the DC bus that feeds the EVs, LTSPICE [21] is used to model and simulate the input and output voltages of step-up converters that serve as a bridge between a solar farm and a DC fast-charging station. Finally, the MPPT approach is simulated using MATLAB® software utilizing the P&O method.

1.1 System configuration

The proposed configuration aims to demonstrate the viability of the suggested system. There are several important parts and components, which can be seen in Fig. 1, that are used when a big solar farm is used to feed an EV charging station with a Level-3, fast-charging capability.

As shown in Fig. 1, the proposed solar farm has PV modules, fast-charging stations, DC–DC converters, power inverters, step-up and step-down transformers, rectifiers, energy meters and a power management system (PMS) [22]. SunPower spr-x22-359 is utilized for this system, which has a very high efficiency. The features of the PV modules used in this investigation are listed in Table 1.

According to the table, the conversion efficiency of the PV modules is 22.03%, the weight of each module is 19.5 kg and the output power of each module is 359.3 W.

1.2 GCR and IRS

The second stage of designing a solar farm is to determine the maximum shadowing situation, which occurs on the December solstice (DS) [23]. At 9 a.m. on the winter solstice, when the shadow is the largest, the elevation angle (α) and azimuth angle (γ) are needed for the GCR calculation [24, 25]. The location of this article is Lubbock, a city located in the north-western region of the state of Texas, in the USA. The latitude and longitude coordinates for Lubbock are 33.5779° N and 101.8552° W, respectively. It is located in the South Plains region, which is characterized by its flat, arid landscape. In terms of climate, Lubbock is classified as having hot summers. The average high temperature (June through August) is ~91°F (33°C), while the average low temperature (December through February) is ~28°F (–2°C). The position of the Sun affects the amount of solar energy that reaches a solar panel, which in turn affects the performance of the panel. The solar geometry for fixed surfaces can be calculated using basic trigonometry. The angle between the Sun and the surface is determined by the altitude and azimuth of the Sun. By calculating the altitude and azimuth of the Sun for a specific location and time of day, the angle between the Sun and the solar panel can be determined. The elevation angle and azimuth angle during the winter solstice in Lubbock at 9 a.m. are depicted in Fig. 2.

Fig. 2 shows the Sun path diagram in Lubbock, which depicts the Sun's path through the sky. This route was created by graphing the azimuth (left–right) and elevation (up–down) angles of the Sun on a specific day. Based on Fig. 2, the azimuth angle at 9 a.m. on the DS is 128° and the elevation angle is 11°. For direct irradiation to reach the other rows, a suitable distance between the rows must be established [27]. Fig. 3 shows the variables required to calculate the highest shadow on the DS.

Based on Fig. 3, for calculating the highest inter-row space, the exact size of each row, the utilized tilt angle and the azimuth and elevation angles of the location are required. The IRS in the winter solstice can be specified by using the following equations:

$$X = Z.\cos(\beta) \tag{1}$$

$$H = Z.\sin(\beta) \tag{2}$$

$$K = \frac{H}{\tan(\alpha)} \tag{3}$$

$$D = K.\sin(\gamma) \tag{4}$$

$$GCR = \frac{X}{X + D} \tag{5}$$

In the above equations, X is the projected width of the array on the ground, Z is the tilted width, H is the height of the array, K is the shadow length, D is the row distance, (α) is the elevation angle, (β) is the tilt angle and (γ) is the azimuth angle. The GCR is the ratio of the solar farm area divided by the ground area [28, 29]. Table 2 shows the module area, ground area, IRS and GCR with the different tilt angles for the proposed solar farm.

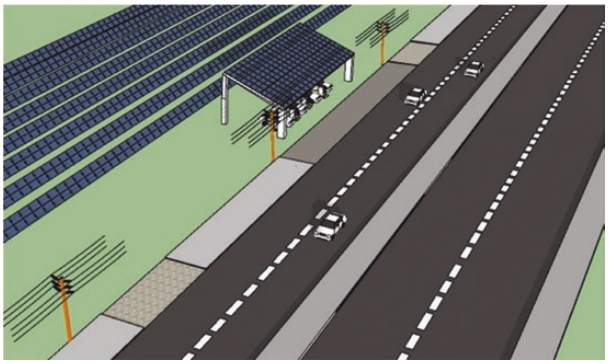

Fig. 1: System configuration

Table 1: PV features

Cells per module	**96**	**Efficiency**	**22.03 %**
Module size	1.5 × 1.04 m	Weight	19.5 kg
Power per module	359.3 W	Tilt	33.5°
Number of modules	2785	Latitude	33.5°
I (SC)	6.51 A	V (OC)	69.6 V
I (MPP)	6.07 A	V (MPP)	59.2 V
Temperature	–40°F to +185°F (–40°C to +85°C)		

SC, short circuit; OC, open circuit.

1.3 Feedback control system

To extract the maximum amount of power and transfer it to the output load, the best converter must be selected [30]. In the proposed feedback control system, the DC–DC step-up converter employing the DMPPT and the P&O method obtain the maximum power from the system.

1.3.1 *Step-up converter*

A DC–DC step-up converter is utilized to boost the voltage of the modules to the proper voltage to achieve the higher desired voltage [31]. The relationship between the duty ratio (D), the inductor (L) and the capacitor (C) of the step-up converter is illustrated below:

$$L = \frac{DV_{pv}T_{sw}}{\Delta I_L} \tag{6}$$

$$C = \frac{DV_O T_{sw}}{R.\Delta V_C} \tag{7}$$

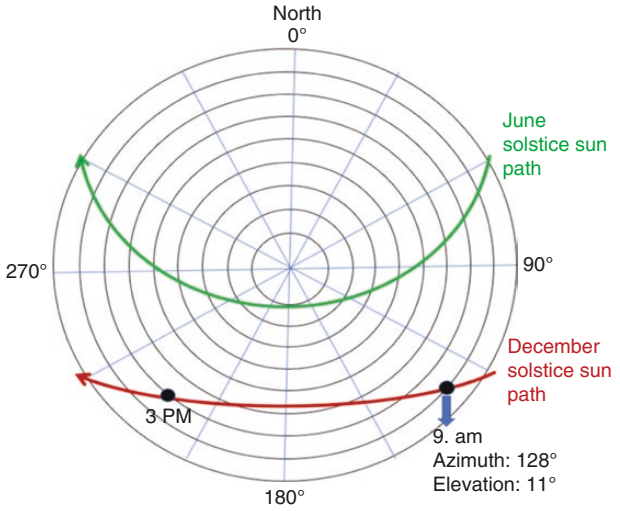

Fig. 2: Sun path diagram indicating the elevation angle and the azimuth angle on the DS [26]

According to Equations (6) and (7), D is the duty ratio, V_{pv} is the PV voltage, T_{sw} is the switching period, ΔI_L is the current ripple of the inductor, V_o is the output, ΔV_C is the voltage ripple of the capacitor and R is the series resistance in the step-up converter [32]. Fig. 4 depicts the step-up converter utilized.

Based on Fig. 4, the step-up converter in use comprises a metal-oxide-semiconductor field-effect transistor (MOSFET), M1, that receives control from an MPPT controller through pulse-width modulation pulses. When M1 is on, the inductor (L1) is charged by the PV module and the current of the inductor increases. On the other hand, when M1 is off, the power coming from the module and the extra stored energy in L1 feed the inverter or the DC fast-charging station through the diode (D1) [33].

1.3.2 *P&O*

Several MPPT approaches may be applied to successfully follow the MPP. The P&O technique is the most famous one due to its fast-tracking feature and accuracy [34]. The P&O control algorithm and the P–V characteristic of the utilized P&O are shown in Fig. 5.

The output power of the PV module changes in response to a slight disturbance, as seen in the P–V curve [35]. The specific parameters used in a P&O algorithm for MPPT can vary depending on the implementation and characteristics of the particular PV system. However, the key parameters typically associated with the P&O algorithm are as follows.

Perturbation step size (0.05): This parameter determines how much the algorithm will change the voltage at each iteration. A smaller step size can lead to more accurate tracking but may slow down convergence, whereas a larger step size can result in faster tracking but potentially overshoot the MPP.

Sampling frequency (100 ms): The algorithm needs to sample the voltage and current of the PV panel at regular intervals to make decisions. The sampling frequency affects the responsiveness of the algorithm and can affect its ability to track rapid changes in environmental conditions. The power output from PV is continuously checked against the previous power and, if there is an increase, the procedure is repeated [36]:

$$\frac{\Delta p}{\Delta v} > 0 \tag{8}$$

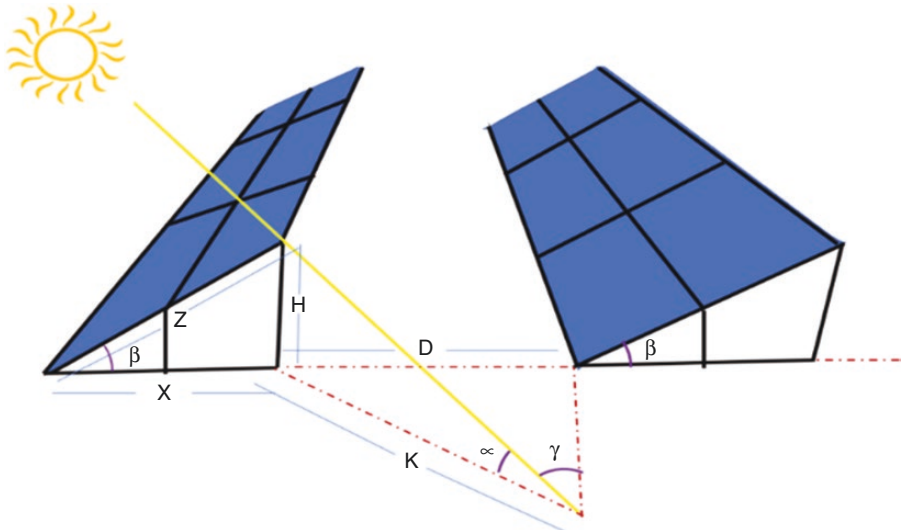

Fig. 3: GCR and IRS in the December solstice

$$\frac{\Delta p}{\Delta v} = 0 \tag{9}$$

$$\frac{\Delta p}{\Delta v} < 0 \tag{10}$$

If $\frac{\Delta p}{\Delta v}$ is positive when using the P&O method, it should continue moving in the same direction until it reaches zero, which is the greatest extracted power. If $\frac{\Delta p}{\Delta v}$ is negative, it should continue moving in the opposite direction until the desired outcome is obtained [37]. In addition, the relevant factors that influence the performance of the P&O algorithm are as follows.

PV parameter variations: The effectiveness of the P&O algorithm is influenced by variations in the parameters of the PV panel, such as temperature, irradiance and age. Temperature variations can significantly affect the P–V curve, shifting the MPP. The algorithm should adapt to these changes by adjusting its perturbation strategy.

Shading conditions: Partial shading of PV panels can create multiple local MPPs, making it difficult for the P&O algorithm to accurately track the global MPP. The algorithm should be designed to handle shading conditions by detecting and avoiding local maxima.

Electrical and thermal losses: Electrical losses in the wiring and components of the PV system, as well as thermal losses in the PV panel, can reduce the overall efficiency of power extraction. The P&O algorithm should be able to compensate for these losses and optimize power output accordingly.

1.3.3 *DMPPT*

The maximum power point of the P–V curve varies as a result of partial shadowing situations, mismatches, time differences and temperature shifts [38]. A DMPPT has been shown to increase the overall effectiveness of PV systems [39]. The DMPPT method is used to reduce the decrease in output power caused by incompatible operation circumstances of the PV module [40]. In this case, a connection that combines parallel and series modules is studied. The fast EV charging station requires a DC voltage of 400 V. A series of PV modules is often connected in series to provide the 400-V level of the charging station to create the appropriate output power and then identical modules are connected in parallel to fit the desired current [41]. Fig. 6 shows the fast EV charging station with DMPPT. In the proposed DMPPT, four modules are connected in series and paralleled with other groups of identical modules using step-up DC–DC converters to provide independent control for each part.

According to Fig. 6, the BSS stores excess solar energy and releases it when needed, ensuring a stable power supply. It can also interact with the grid, exporting excess energy to optimize energy usage. In addition, the grid-connected inverter converts solar-generated DC electricity into AC electricity, making it usable to be fed to the power grid. It syncs with the grid and allows surplus energy to be fed back, enhancing energy efficiency and potentially reducing electricity costs.

Table 2: IRS and GCR with different tilt angles

	β = 15°	β = 20°	β = 25°	β = 30°	β = 33.5°
IRS = *D*	1.032 m	1.4 m	1.73 m	2.07 m	2.27 m
GCR	0.48	0.4	0.34	0.29	0.26
Module area	4174 m²	4174 m²	4174 m²	4174 m²	4174 m²
Ground area	6344 m²	6678 m²	6928 m²	7137 m²	7262 m²

1.4 Level-3 charging station

There are now three different levels of EV charging: Level 1, Level 2 and Level 3 [42]. The power output from the charging station determines which of the three EV charging levels is used. The maximum output for Level-1 charging stations is <5 kW, making it the slowest method of charging an electric car. With a power limit just below 25 kW, a Level-2 charging station may charge an EV more quickly than a Level-1 charger. The most powerful charging stations available today, Level-3 chargers, can supply upward of 100 kW of electric power [43]. Level-3 charging is ideal for cities along streets such as gas stations due to the speed with which it charges [44]. An on-board charger is used for Level-1 and Level-2 charging to convert power from AC into DC. For Level-3 charging, the conversion takes place in an EV fast-charging station and not in the vehicle. Therefore, Level-3 charging stations are faster and can provide electricity at higher rates. For example, a Level-3 charger can charge an EV in <1 hour at its maximum power output [45]. However, the use of a lot of electricity from

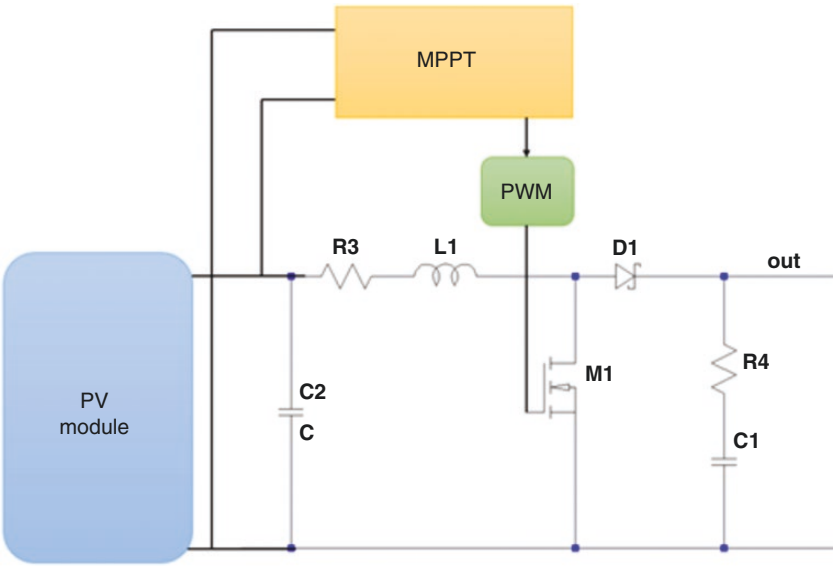

Fig. 4: Utilized step-up converter

the power grid places a lot of stress on the power grid feeders [46]. Therefore, when talking about a significant number of EVs, the only option is to use renewable energy such as solar. Fig. 7 indicates the fast EV station that uses solar energy coming from a proposed 1-MW PV system.

Fig. 7 shows four DC fast-charging stations between EVs. Each of the DC fast-charging stations has an off-board EV charger that uses step-up DC–DC converters to power the DC bus, which in turn powers the EVs. The output voltage of the solar farm is DC voltage; therefore, by using DC–DC step-up converters, solar energy can be used to power EVs using the recommended DC fast-charging station without the need for equipment to convert AC voltage into DC [47].

1.5 BSS

To offer a stable output of the designed 1-MW PV system, a BSS is required in conjunction with a solar system due to the intermittent nature of PV energy [48]. The BSS used is a lithium-ion battery with a rated capacity of 26 V and 180 Ah, offering a DoD of 80%, 96% efficiency and an impressive cycle life of 10 000 cycles. This integration improves the stability of the system, enabling an uninterrupted power supply for EV charging while efficiently using solar energy. When the PV output is greater than the demand, the BSS can be charged and the extra energy can be saved. Regarding the design, the BSS must be between the PV farm and the EV station. A safety concern may arise if the EV load is accompanied by shutdown interruptions caused by the extremely high fluctuations of the PV power supply. To solve the problem mentioned above, a battery may buffer the power output of PV energy, allowing EVs to charge considerably more smoothly [49]. When deploying PV energy for a public EV charging station, at noon, the battery stores any extra PV energy that might be released if the PV output is unexpectedly interrupted, especially due to cloud cover. Fig. 8 depicts the general configuration and output power of the system with a buffer storage system. The output power of the system is simulated using SAM software, as shown in Fig. 8b.

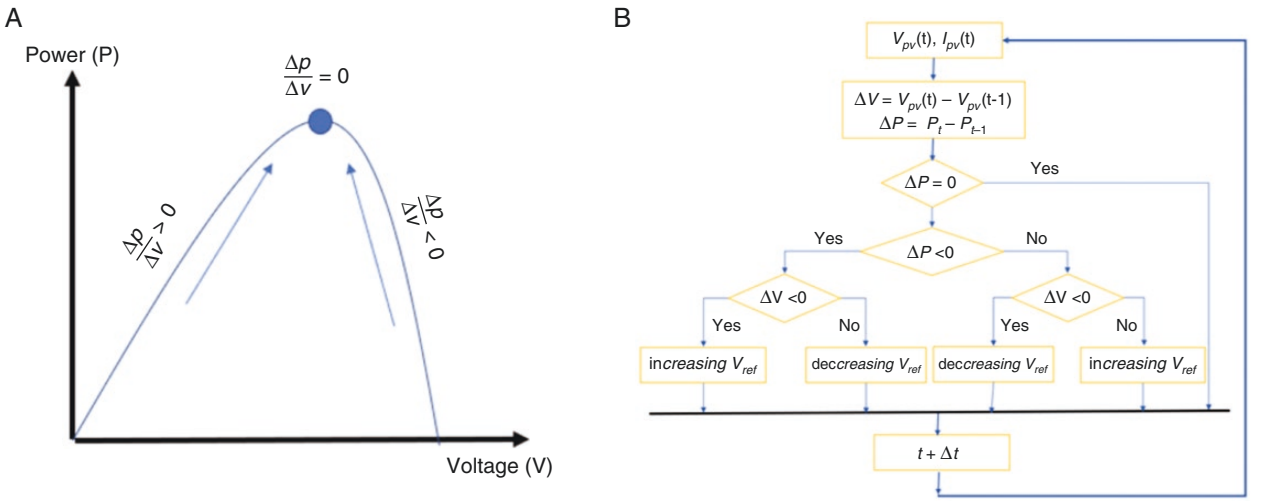

Fig. 5: P&O. (a) P–V characteristic of the utilized P&O method; (b) P&O control algorithm.

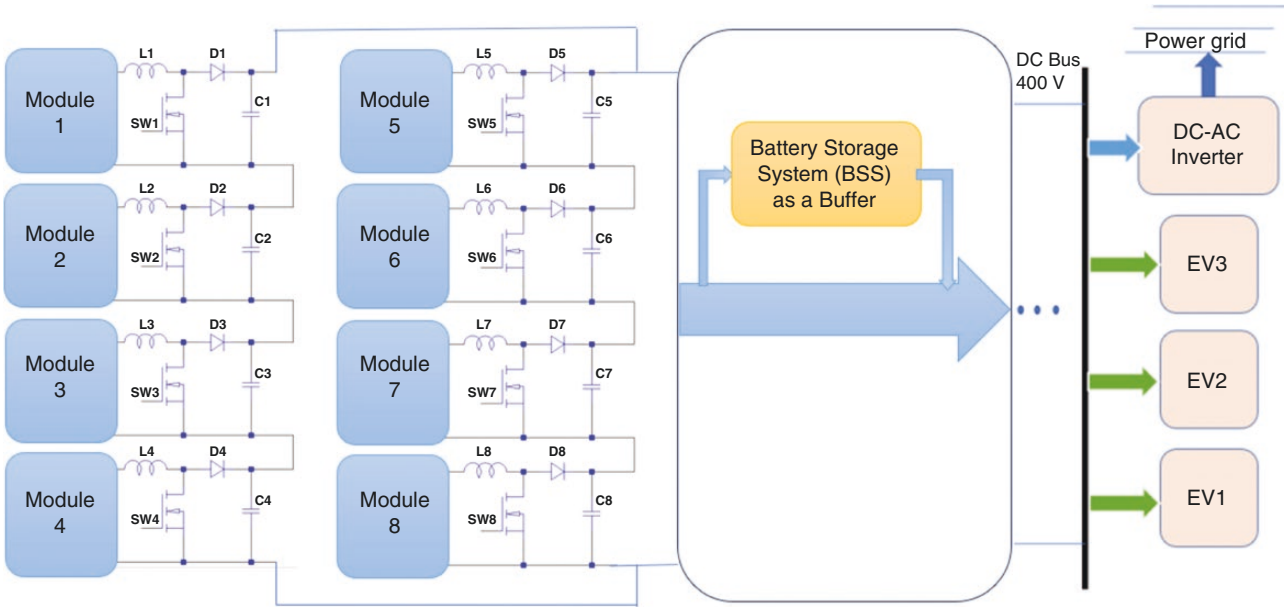

Fig. 6: Proposed DMPPT structure

According to Fig. 8, P_{EV} stands for the power required to charge each EV without interruption. However, because solar energy is intermittent, the actual output power of a PV system looks like the blue part of the figure, which is generated using SAM software. As a result, at the moment of PV interruption, P_{EV} cannot be acquired continuously and a buffer storage system is required for a very short period of time to smooth the output power to obtain a continuous charge output from the EV station.

2 Results and discussion

In this research, the 1-MW solar system connected to the EV charging station and the connected inverter to the grid are studied and the system was modelled by using MATLAB®, LTSPICE and SAM software.

2.1 Results

The performance of the proposed solar-powered charging station system is evaluated through simulations under various operating conditions. This paper aims to address inherent challenges in solar power generation, including solar irradiation, weather conditions, solar array mismatches and partial shading conditions. To maximize power extraction from the proposed 1-MW solar farm, a DMPPT technique is implemented. DMPPT, particularly when applied to each individual module, demonstrated the highest efficiency in overcoming mismatches and shading. Temperature was found to have a big impact on the amount of power a PV system produces. Module temperature and ambient temperature are two different variables regarding a PV system. In order to depict the module and ambient temperature, SAM is utilized. Fig. 9 shows the average ambient and cell temperatures throughout the course of the year in Lubbock, Texas.

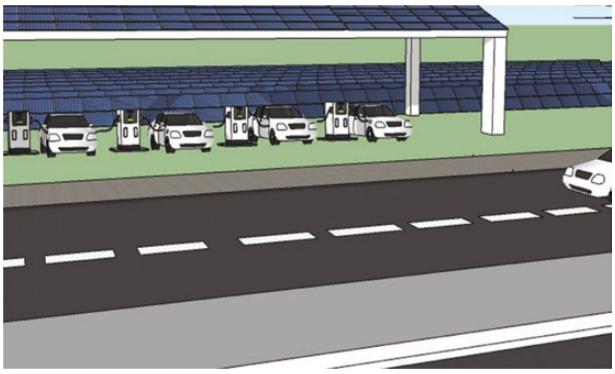

Fig. 7: DC fast EV station

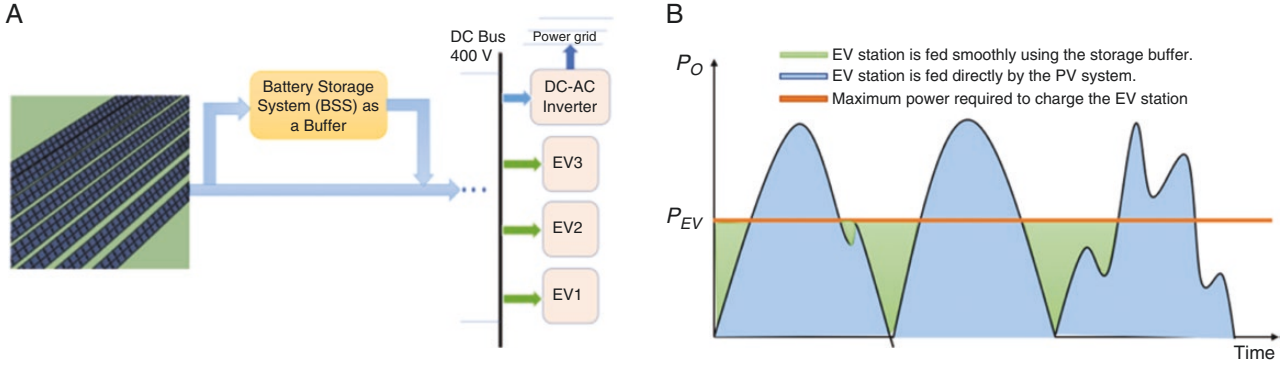

Fig. 8: (a) General configuration of the system with a buffer storage system and (b) smooth required power

The highest module temperature was recorded in July, as shown in Fig. 9. The module temperature is highest while the PV system is generating power. The highest ambient temperature in Lubbock is ~40°C, whereas the maximum cell temperature is ~70°C. Fig. 10 depicts the voltage simulation of the step-up converters that are employed to increase the output voltage of the system and are essential for increasing the output voltage to the industry-standard 400 V for EV charging.

To reach the 400-V level, four PV modules in series are connected, which maximize efficiency, system reliability and precise voltage regulation. The output voltage of the modules may be increased to the appropriate voltage for the EVs by connecting four modules in series and using one step-up converter for each module. This approach enables the fast and seamless charging of EVs while maintaining the stability and safety of the charging process. Also, Fig. 11 shows the thorough examination of the inductor current of a single boost converter that is in continuous conduction mode (CCM). The CCM mode is a critical operational state for power electronics converters such as boost converters, particularly in the context of our solar-powered EV charging station.

In CCM mode, the inductor current experiences continuous and steady flow throughout the entire switching cycle. Unlike the discontinuous conduction mode, in which the inductor current drops to zero during part of the cycle, CCM maintains a non-zero current. This mode offers several advantages. First, it contributes to higher efficiency in power conversion, as there is no current discontinuity, resulting in reduced switching losses. Furthermore, CCM provides better voltage regulation, ensuring that the output voltage remains stable even under varying loads. The most important benefit of using solar energy is that summer is when both solar power generation and consumption are at their peak.

Due to greater peak Sun hours and fewer overcast days, monthly energy output is higher during the summer months, as illustrated in Fig. 12. Based on Fig. 12, the highest extracted power with the system occurs in July, with 170 MWh of power production. A heat map of the generated electricity throughout the course of the year is shown in Fig. 13. The 365 days can be viewed on the top and the 24 hours every day can be seen on the left-hand side. The red regions denote the periods of peak electricity generation.

The highest extracted power of the system is 869 kW, which can be seen from Fig. 13. Furthermore, Fig. 14, indicates the hourly energy production of the presented system.

In Fig. 14, an hour-by-hour breakdown of the rated DC output power of the proposed solar-based EV charging system is simulated. This detailed analysis takes into account various system losses, including dust accumulation, wire connection losses and

other factors. The findings indicate that, under ideal conditions, the system can produce an impressive maximum power output of nearly 900 kW per hour. However, it is important to note that this figure accounts for the inherent losses that occur in any real-world system. These losses are often attributed to factors such as dust accumulation on solar panels, resistive losses in wiring and other inefficiencies. To determine the number of EVs that can be charged with this level of power output, on average, a proposed

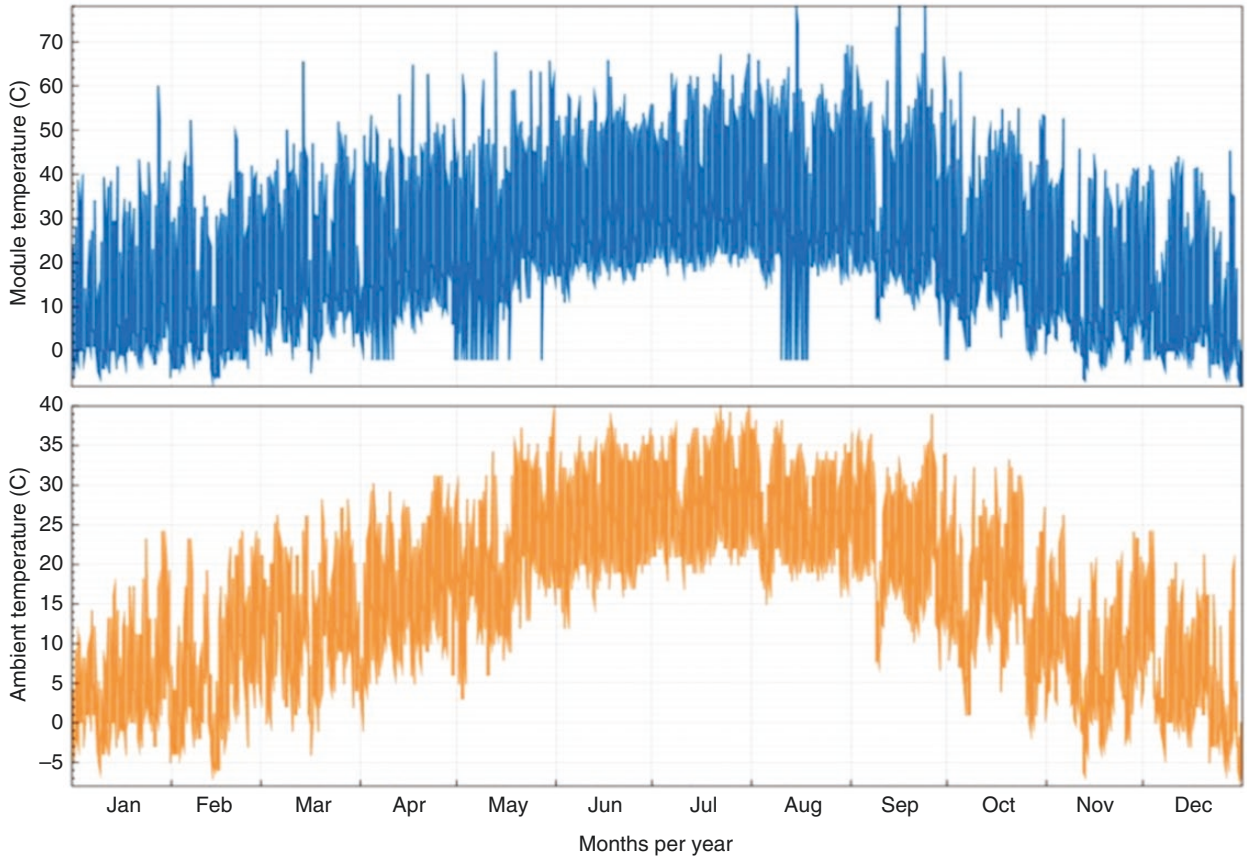

Fig. 9: Ambient temperature versus module temperature

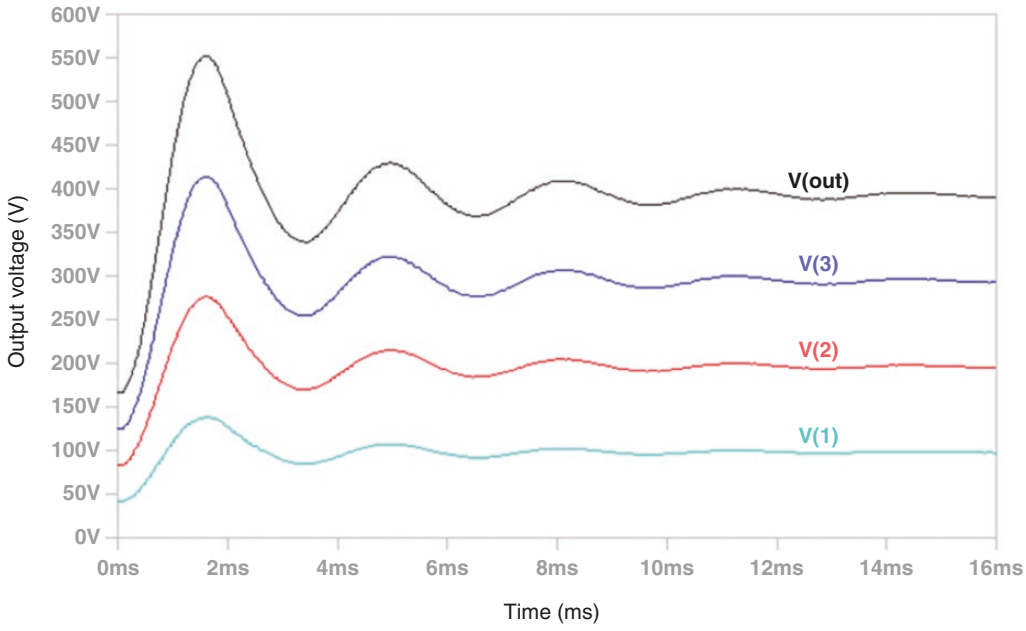

Fig. 10: Output voltage of the boost converters in series

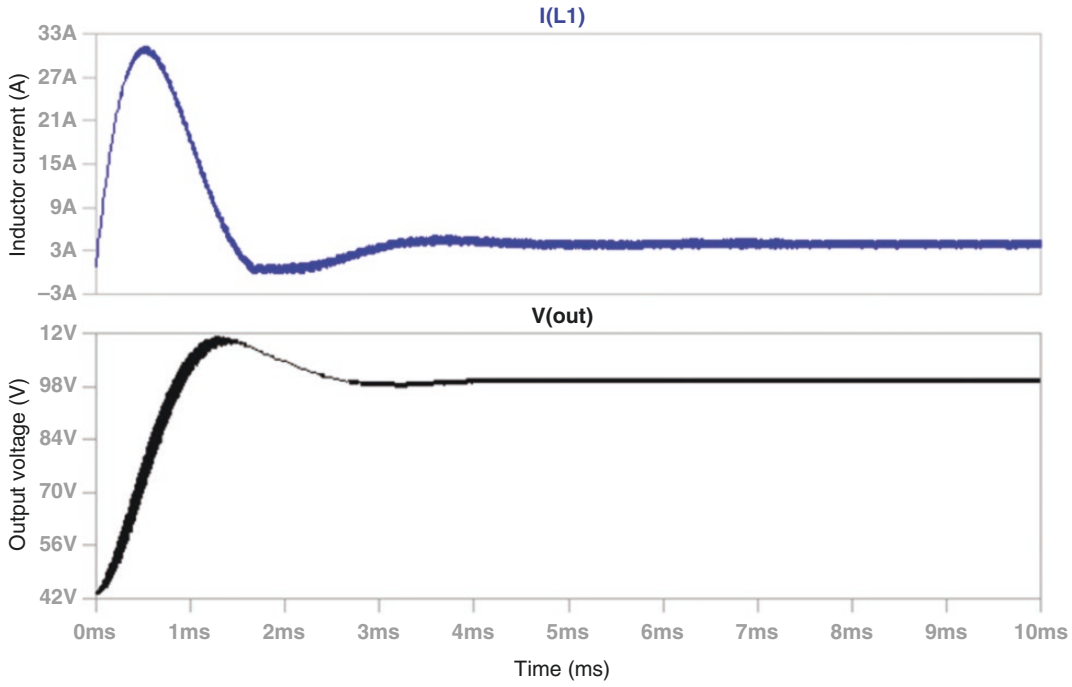

Fig. 11: Inductor current in CCM mode

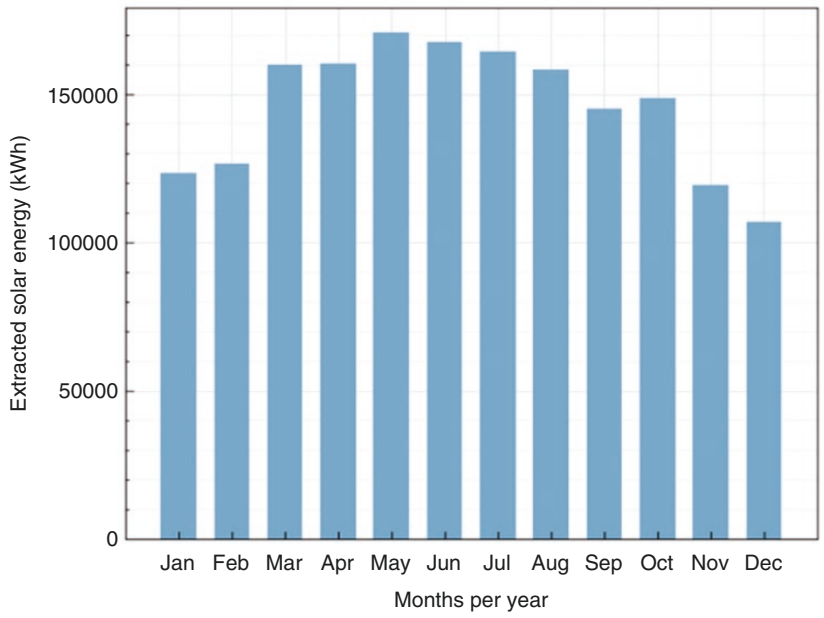

Fig. 12: Monthly extracted solar energy

Level-3 DC fast charger can provide ~50–120 miles of range per hour of charging, depending on the EV model and battery capacity.

2.2 Discussion

This paper proposes the use of a DMPPT technique to reduce the reduction in output power caused by mismatch problems. This technique allows real-time tracking of the maximum power point of the solar panels, even when they are not identical in characteristics, thus maximizing the power output and reducing the impact of mismatch losses. By reducing the impact of mismatch losses, the proposed technique can help to increase the overall efficiency of the system and maximize the use of the available solar energy. This paper also suggests that using a solar-powered DC fast EV charging station can help to reduce the system cost in the long run. The use of solar energy as a source of power can help to reduce dependence on the electricity grid, thereby reducing the electricity bills associated with operating the charging station. Furthermore, the study proposes the use of high-efficiency solar panels and an optimal number of panels, which can help to further reduce the cost of the solar system. In addition, this paper proposes a simple and straightforward design for the DC fast EV charging station, which can reduce the complexity of the system. The proposed design uses a boost converter topology, which reduces the number of components required for the charging station, simplifies the control system and reduces the

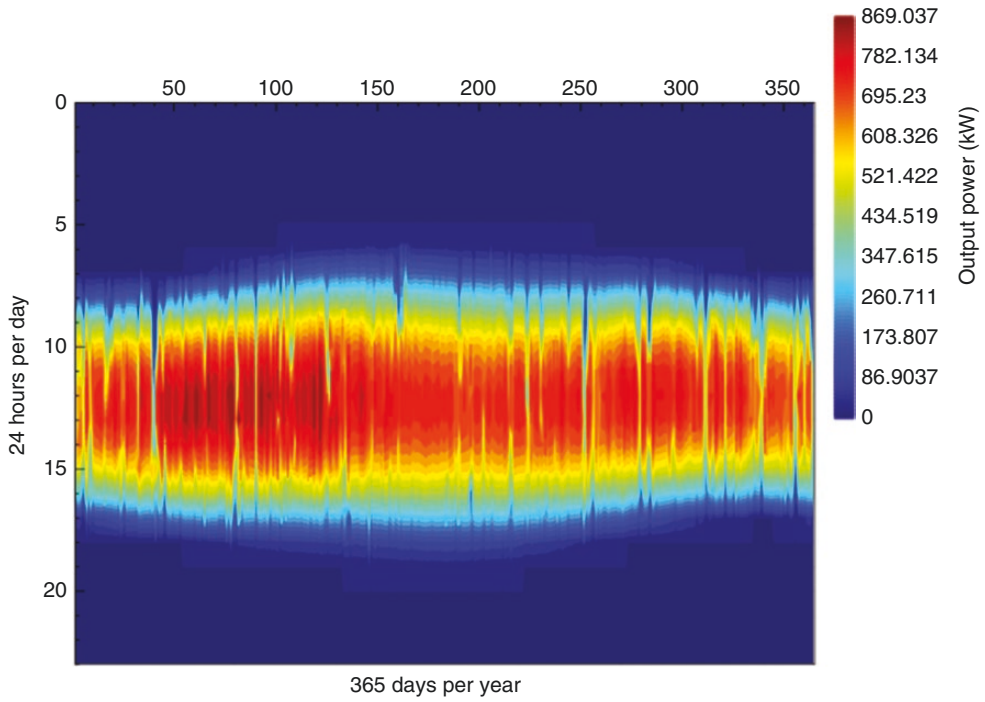

Fig. 13: Heat map of the 1-MW solar power

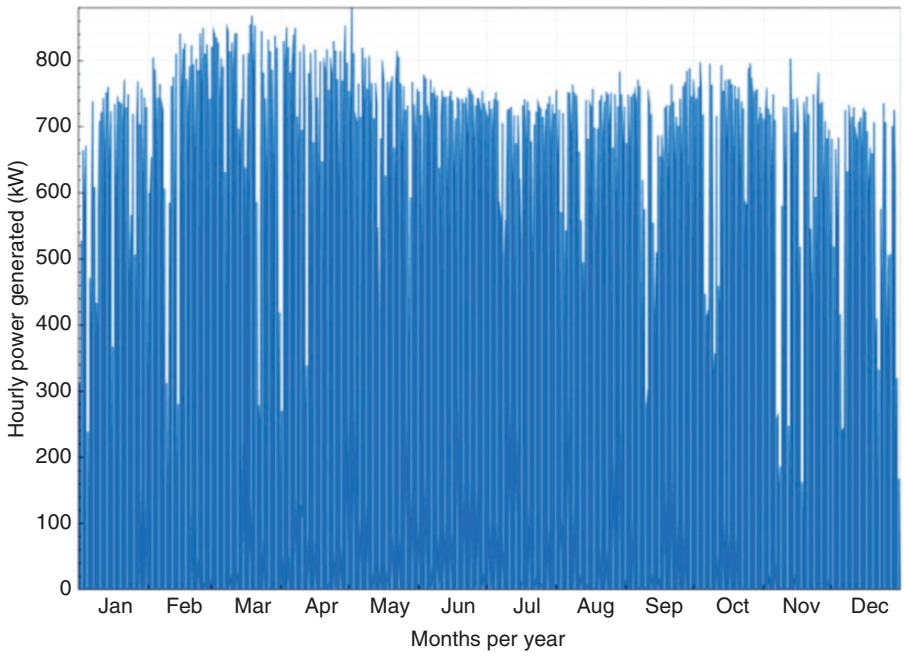

Fig. 14: Rated DC output power per hour

overall complexity of the system. This simplified design can reduce the cost of the charging station and make it easier to install and maintain. Finally, the use of solar energy as a power source for the DC fast EV charging station can help to eliminate a significant amount of toxic gases such as CO_2 and SO_2. By reducing the dependence on fossil fuels and grid electricity, the charging station can help to reduce the carbon footprint associated with EV charging, which is an important step towards achieving a sustainable and zero-emission transportation system. For example, the average amount CO_2 released by coal-fired power plants per kilowatt hour of electricity is 2.21 pounds, increasing the chance of climate change and contributing to smog, acid rain and haze. Under ideal conditions, the proposed system has the ability to generate 900 kW per hour. Consequently, this results in the removal of $2.21 \times 900 = 1989$ pounds of CO_2 from the atmosphere every hour compared with coal-fired power plants.

3 Conclusion

In this paper, a 1-MW solar system is studied connected to an EV charging station and grid-connected inverter, and the system was modelled using MATLAB®, LTSPICE and SAM software. It has also

been demonstrated that a DMPPT improves the overall effectiveness of PV systems. The DMPPT technique is utilized to reduce the reduction in output power caused by unfavourable working conditions of the PV module, such as mismatch problems. Additionally, a fast EV charging station is built to directly use the DC voltage of the suggested solar system, reducing the cost and complexity of the system. The planned 1-MW solar system generates 5 MWh of electricity daily, which is enough to completely charge ~120 BEVs every day. In addition, utilizing the suggested PV system helps the environment by eliminating a significant quantity of greenhouse gases and toxic gases, including SO_2 and CO_2. For example, compared with coal-fired power plants, the method discussed in this article will remove 1989 pounds of CO_2 from the air hourly. Because the data collected were from one geographic location, the generalizability of the findings is limited. Furthermore, the analysis only looked at solar energy, but adding wind energy to the system might make it much more viable. Future studies should focus on overcoming these restrictions and expanding the model to various regions by incorporating wind energy.

Acknowledgements

In this work, the financial support of the National Science Foundation (NSF) under Award Number: 2115427 is gratefully acknowledged. SRS RN: Sustainable Transportation Electrification for an Equitable and Resilient Society (STEERS).

Conflict of interest statement

None declared.

Data Availability

The data used in this article are available in the SAM software, which provides access to data for various locations. There is no specific repository or DOI link for these data as they are integrated directly into the SAM software.

References

[1] Sanguesa J, Torres-Sanz V, Garrido P, *et al*. A review on electric vehicles: technologies and challenges. *Smart Cities*, 2021, 4:372–404.

[2] Wang L, Qin Z, Slangen T, *et al*. Grid impact of electric vehicle fast charging stations: trends, standards, issues and mitigation measures-an overview. *IEEE Open J Power Electron*, 2021, 2:56–74.

[3] Ul-Haq A, Buccella C, Cecati C, *et al*. Smart charging infrastructure for electric vehicles. In: *2013 International Conference on Clean Electrical Power (ICCEP)*, Alghero, Italy, 11–13 June 2013, 163–169.

[4] Alkawsi G, Baashar Y, Abbas D, *et al*. Review of renewable energy-based charging infrastructure for electric vehicles. *Appl Sci*, 2021, 11:3847.

[5] Piekut M. The consumption of renewable energy sources (RES) by the European Union households between 2004 and 2019. *Energies*, 2021, 14:5560.

[6] Energy Information Agency (EIA). *The United States consumed a record amount of renewable energy in 2019*. 2020. https://www.eia.gov/todayinenergy/detail.php?id=45516 (30 November 2023, date last accessed).

[7] Yu J, Tang Y, Chau K, *et al*. Role of solar-based renewable energy in mitigating CO_2 emissions: evidence from quantile-on-quantile estimation. *Renew Energy*, 2022, 182:216–226.

[8] Lodin O, Kaur I, Kaur H. Predictive-P&O MPPT algorithm for fast and reliable tracking of maximum power point in solar energy systems. *Int J Recent Technol Eng*, 2019, 7:264–268.

[9] Pathipati V, Azeez N, Williamson S. Standalone DC level-1 EV charging using PV/grid infrastructure, MPPT algorithm and CHAdeMO protocol. In: *IECON 2015—41st Annual Conference of the IEEE Industrial Electronics Society*, Yokohama, Japan, 9–12 November 2015, 005408–005414.

[10] Fathabadi H. Novel grid-connected solar/wind powered electric vehicle charging station with vehicle-to-grid technology. *Energy*, 2017, 132:1–11.

[11] Atawi I, Hendawi E, Zaid S. Analysis and design of a standalone electric vehicle charging station supplied by photovoltaic energy. *Processes*, 2021, 9:1246.

[12] Awad M, Ibrahim A, Alaas Z. Design and analysis of an efficient photovoltaic energy-powered electric vehicle charging station using perturb and observe MPPT algorithm. *Front Energy Res*, 2022, 10:969482.

[13] Singh S, Chauhan P, Singh N. Feasibility of grid-connected solar-wind hybrid system with electric vehicle charging station. *J Mod Power Syst Clean Energy*, 2020, 9:295–306.

[14] Zhang Y, He J, Ionel D. Modeling and control of a multiport converter based EV charging station with PV and battery. In: *2019 IEEE Transportation Electrification Conference and EXPO (ITEC)*, Detroit, USA, 19–21 June 2019, 1–5.

[15] Wang F, Zhu T, Zhuo F, *et al*. Analysis and comparison of FPP and DPP structure based DMPPT PV system. In: *2016 IEEE 8th International Power Electronics and Motion Control Conference (IPEMC-ECCE Asia)*, Hefei, China, 22–26 May 2016, 207–211.

[16] Jiang J, Zhang T, Chen D. Analysis, design, and implementation of a differential power processing DMPPT with multiple buck–boost choppers for photovoltaic module. *IEEE Trans Power Electron*, 2021, 36:10214–10223.

[17] Yetayew T, Jyothsna T, Kusuma G. Evaluation of by-pass diode and DMPPT under partial shade condition of photovoltaic systems. In: *2017 7th International Conference on Power Systems (ICPS)*, Pune, India, 21–23 December 2017, 31–36.

[18] Oulad-Abbou D, Doubabi S, Rachid A, *et al*. Combined control of MPPT, output voltage regulation and capacitors voltage balance for three-level DC/DC boost converter in PV-EV charging stations. In: *2018 International Symposium on Power Electronics, Electrical Drives, Automation and Motion (SPEEDAM)*, Amalfi, Italy, 20–22 June 2018, 372–376.

[19] Ahmadi M, Kaleybar H, Brenna M, *et al*. DC railway micro grid adopting renewable energy and EV fast charging station. In: *2021 IEEE International Conference on Environment and Electrical Engineering and 2021 IEEE Industrial and Commercial Power Systems Europe (EEEIC/I&CPS Europe)*, Bari, Italy, 7–10 September 2021, 1–6.

[20] Freeman J, DiOrio N, Blair N, *et al*. *System Advisor Model (SAM) General Description (Version 2017.9. 5)*. Golden, CO, USA: National Renewable Energy Laboratory (NREL), 2018.

[21] Mikkelsen J. *LTSPICE–An Introduction, Technical Report*. Aalborg, Denmark: Institute of Electronic Systems, Aalborg University, 2005.

[22] Dellosa J, Panes M, Espina R. Techno-economic analysis of a 5 MWp solar photovoltaic system in the Philippines. In: *2021 IEEE International Conference on Environment and Electrical Engineering and 2021 IEEE Industrial and Commercial Power Systems Europe (EEEIC/I&CPS Europe)*, Bari, Italy, 7–10 September 2021, 1–6.

[23] Balal A, Herrera M, Johnson E, *et al*. Design and simulation of a solar PV system for a university building. In: *2021 IEEE 4th International Conference on Power and Energy Applications (ICPEA)*, Busan, Korea, 9–11 October 2021, 122–125.

[24] Chen X, Yang X. Solar collector with asymmetric compound parabolic concentrator for winter energy harvesting and summer overheating reduction: concept and prototype device. *Renew Energy*, 2021, 173:92–104.
[25] Kafka J, Miller M. The dual angle solar harvest (DASH) method: an alternative method for organizing large solar panel arrays that optimizes incident solar energy in conjunction with land use. *Renew Energy*, 2020, 155:531–546.
[26] Balal A, Dallas T. The influence of tilt angle on output for a residential 4 kW solar PV system. In: *2021 IEEE 4th International Conference on Power and Energy Applications (ICPEA)*, Busan, Korea, 9–11 October 2021, 131–134.
[27] Braun J, Mitchell J. Solar geometry for fixed and tracking surfaces. *Sol Energy*, 1983, 31:439–444.
[28] Mokhtara C, Negrou B, Settou N, *et al*. Optimal design of grid-connected rooftop PV systems: an overview and a new approach with application to educational buildings in arid climates. *Sustainable Energy Technol Assess*, 2021, 47:101468.
[29] Varga N, Mayer M. Model-based analysis of shading losses in ground-mounted photovoltaic power plants. *Sol Energy*, 2021, 216:428–438.
[30] Koç Y, Birbir Y, Bodur H. Non-isolated high step-up DC/DC converters: an overview. *Alex Eng J*, 2022, 61:1091–1132.
[31] Athikkal S, Chokkalingam B, Ganesan S, *et al*. Performance evaluation of a dual-input hybrid step-up DC–DC converter. *IEEE Trans Ind Appl*, 2022, 58:3769–3782.
[32] Basha C, Murali M. A new design of transformerless, non-isolated, high step-up DC-DC converter with hybrid fuzzy logic MPPT controller. *Int J Circuit Theory Appl*, 2022, 50:272–297.
[33] Balal A, Giesselmann M. PV to vehicle, PV to grid, vehicle to grid, and grid to vehicle micro grid system using level three charging station. In: *2022 IEEE Green Technologies Conference (GreenTech)*, IEEE: Houston, TX, USA, 30 March 2022–01 April 2022, 25–30.
[34] Balal A, Abedi M, Shahabi F. Optimized generated power of a solar PV system using an intelligent tracking technique. *Int J Power Electron Drive Syst*, 2021, 12:2580.
[35] Abouadane H, Fakkar A, Sera D, *et al*. Multiple-power-sample based P&O MPPT for fast-changing irradiance conditions for a simple implementation. *IEEE J Photovoltaics*, 2020, 10:1481–1488.
[36] Mamarelis E, Petrone G, Spagnuolo G. A two-steps algorithm improving the P&O steady state MPPT efficiency. *Appl Energy*, 2014, 113:414–421.
[37] Osman M, Refaat A. Adaptive multi-variable step size P&O MPPT for high tracking-speed and accuracy. *Mater Sci Eng*, 2019, 463:012050.
[38] Solórzano J, Egido M. Hot-spot mitigation in PV arrays with distributed MPPT (DMPPT). *Sol Energy*, 2014, 101:131–137.
[39] Yuan J, Zhao Z, Liu Y, *et al*. DMPPT control of photovoltaic microgrid based on improved sparrow search algorithm. *IEEE Access*, 2021, 9:16623–16629.
[40] Kumar K, Varshney L, Ambikapathy A, *et al*. Solar tracker transcript: a review. *Int Trans Electr Energy Syst*, 2021, 31:13250.
[41] Elma O. A dynamic charging strategy with hybrid fast charging station for electric vehicles. *Energy*, 2020, 202:117680.
[42] Sears J, Roberts D, Glitman K. A comparison of electric vehicle Level 1 and Level 2 charging efficiency. In: *2014 IEEE Conference on Technologies for Sustainability (SusTech)*, Portland, USA, 24–26 July 2014, 255–258.
[43] Srdic S, Lukic S. Toward extreme fast charging: challenges and opportunities in directly connecting to medium-voltage line. *IEEE Electrif Mag*, 2019, 7:22–31.
[44] Lin H, Bian C, Wang Y, *et al*. Optimal planning of intra-city public charging stations. *Energy*, 2022, 238:121948.
[45] Sachan S, Deb S, Singh P, *et al*. A comprehensive review of standards and best practices for utility grid integration with electric vehicle charging stations. *Wiley Interdiscip Rev Energy Environ*, 2022, 11:424.
[46] Dharmakeerthi C, Mithulananthan N, Saha T. Impact of electric vehicle fast charging on power system voltage stability. *Int J Electr Power Energy Syst*, 2014, 57:241–249.
[47] Balal A, Dinkhah S, Shahabi F, *et al*. A review on multilevel inverter topologies. *Emerg Sci J*, 2022, 6:185–200.
[48] Huang C, Zhang H, Song Y, *et al*. Demand response for industrial micro-grid considering photovoltaic power uncertainty and battery operational cost. *IEEE Trans Smart Grid*, 2021, 12:3043–3055.
[49] Alam M, Muttaqi K, Sutanto D. Battery energy storage to mitigate rapid voltage/power fluctuations in power grids due to fast variations of solar/wind outputs. *IEEE Access*, 2021, 9:12191–12202.